

INNOVATIVE CLINICAL IMAGE

Hemosiderin Detection inside the Mammillary Bodies Using Quantitative Susceptibility Mapping on Patients with Wernicke-Korsakoff Syndrome

Yuri Nakamura¹, Yasutaka Fushimi^{1*}, Takuya Hinoda¹, Satoshi Nakajima¹,
Akihiko Sakata¹, Sachi Okuchi¹, Sayo Otani¹, Hiroshi Tagawa¹,
Yang Wang¹, Satoshi Ikeda¹, Hirotsugu Kawashima², Maiko T Uemura³,
and Yuji Nakamoto¹

Hemorrhage inside the mammillary bodies (MMBs) is known to be one of the findings of Wernicke encephalopathy. Brain MRI of two patients with Wernicke-Korsakoff syndrome (WKS) demonstrated high susceptibility values representing hemosiderin deposition in MMBs by using quantitative susceptibility mapping (QSM). QSM provided additional information of susceptibility values to susceptibility-weighted imaging in diagnosis of WKS.

Keywords: *mammillary body, quantitative susceptibility mapping, Wernicke-Korsakoff syndrome*

Introduction

Wernicke encephalopathy (WE) is a neurological disease typically characterized by the triad of conscious disturbance, gait disturbance, and eye-movement disorder.¹ WE often requires emergent treatment for acute neurologic morbidity; however, some patients with WE showed the ambiguous onset, and if prompt treatment is not conducted, they will suffer from permanent brain damage known as Korsakoff syndrome (KS).²⁻³ The pathophysiology of WE is thought to be cytotoxic and vasogenic edema due to dysfunction of the Krebs cycle and the pentose phosphate pathway.²⁻⁴ Typical findings of WE are high-intensity lesions on fluid-attenuated inversion-recovery (FLAIR) which may appear in bilateral periventricular regions of the thalamus, hypothalamus, mammillary bodies (MMBs), and periaqueductal regions. Contrast enhancement in the MMBs is also known to be

the finding of WE, and the breakdown of blood brain barrier leads to the hemorrhage inside MMBs. High-resolution MRI including susceptibility weighted imaging (SWI) is helpful for detection of hemosiderin deposition in MMBs.⁵⁻⁶

Quantitative susceptibility mapping (QSM) is a robust technique for quantitative measurement of magnetic susceptibility. QSM is calculated from raw phase and magnitude images of gradient echo images; diamagnetic and paramagnetic substances cannot be distinguished on SWI and T2*-weighted images.⁷ By using QSM, we can differentiate diamagnetic substances, such as calcification and myelin, from paramagnetic substances, such as ferritin and hemosiderin.⁷⁻⁸ QSM demonstrated increased susceptibility in gadolinium deposition,⁹ Alzheimer's disease,^{10,11} and applied into various clinical situations.¹²

QSM findings of two cases with Wernicke-Korsakoff syndrome (WKS) are reported in this study, and susceptibility values of MMBs are compared between patients with WKS and age-matched patients without any intracranial lesions.

Methods

Cases with WKS

Case 1. A 55-year-old male with subacute progressive dementia was referred to our hospital for endoscopic sphincterotomy to remove common bile duct stone. He also suffered from alcoholic liver cirrhosis with mild hepatic encephalopathy. He was found to have cognitive impairment on the rounds, and blood sampling showed low serum thiamine. Rapid administration of thiamine did not improve his cognitive impairment. A brain MRI was performed on the 11th admission day.

¹Department of Diagnostic Imaging and Nuclear Medicine, Graduate School of Medicine, Kyoto University, Kyoto, Kyoto, Japan

²Department of Psychiatry, Graduate School of Medicine, Kyoto University, Kyoto, Kyoto, Japan

³Departments of Neurology, Graduate School of Medicine, Kyoto University, Kyoto, Kyoto, Japan

*Corresponding author: Department of Diagnostic Imaging and Nuclear Medicine, Graduate School of Medicine, Kyoto University, 54 Shogoin Kawahara-cho, Sakyo-ku, Kyoto, Kyoto 606-8507, Japan. Phone: +81-75-751-3760, Fax: +81-75-771-9709, E-mail: yfushimi@kuhp.kyoto-u.ac.jp



This work is licensed under a Creative Commons Attribution-NonCommercial-NoDerivatives International License.

©2022 Japanese Society for Magnetic Resonance in Medicine

Received: August 31, 2022 | Accepted: November 1, 2022

Case 2. A 52-year-old male was hospitalized with difficulty in body movement and disturbance of consciousness. He had been a heavy drinker for several years and was diagnosed as liver cirrhosis, and his family was aware of the patient's cognitive decline and gait disturbance for 3 months prior to admission. On admission, he had ocular deviation; neurological examination showed disorientation and attenuated tendon reflexes. Both serum thiamine and folate acid turned out to be low. His conscious disturbance improved slightly immediately after thiamine injection temporarily; however, it soon deteriorated. A brain MRI was performed on the 6th admission day.

Patients (Control)

SWI is clinically useful for evaluating deposition of hemosiderin, iron, and calcification, and MR scans including SWI are often used in our hospital to diagnose or to rule out cerebrovascular diseases, neurodegenerative diseases, and dementia. Male patients who were between 50 and 58 years old without any severe central nervous diseases from January 2017 to June 2022 and who underwent SWI and QSM, created from the corresponding magnitude and raw phase data, were retrospectively enrolled in this study. Eleven patients were included and our institutional review board approved this study and written informed consent was waived.

MR imaging

All MR examinations were performed at a 3T scanner (MAGNETOM Skyra; Siemens Healthineers, Erlangen, Germany) with 32-channel head coil. MRI protocol included a 3D axial gradient echo (GRE) sequence with the following imaging parameters: TR/TE, 28/20 msec; FOV, 179 × 230 mm; resolution, 0.72 × 0.72 mm; slice thickness, 1.0 mm; and generalized autocalibrating partially parallel acquisitions, 2×. SWI was automatically created after acquisition of 3D GRE images on the MR console. Raw phase data were retrospectively reconstructed from 3D GRE images by using retro-recon function. FLAIR, diffusion weighted imaging (DWI), and MR angiography (MRA) were also performed.

Post-imaging analysis

QSM was calculated from the magnitude and phase images of the 3D GRE images with STI Suite ver.3 (<https://people.eecs.berkeley.edu/~chunlei.liu/software.html>). Phase unwrapping and background phase removal were performed by using brain mask images created from the magnitude image using skull stripping tool. After background phase removal, susceptibility map was calculated from the resulting local tissue phase image by solving an inverse problem using the algorithm for sparse linear equations and least squares (iLSQR method).

ROI analysis was performed as follows: one rater (Y.N., 2 years of experience in radiology) placed ROIs on the magnitude images manually around the contours of each region,

and approved by another rater (Y.F., 24 years of experience in neuroradiology). Then, ROIs were transferred to QSM, and susceptibility values of bilateral MMB, globus pallidus, putamen, substantia nigra, and red nucleus were measured.

Results

Brain MRI showed moderate brain atrophy in both cases. SWI showed low-intensity spots in both MMBs in both cases with WKS. QSM showed high susceptibility values corresponding to the lesions of MMBs, which suggests paramagnetic susceptibility such as hemosiderin (Fig. 1). FLAIR showed no hyperintensities in bilateral periventricular regions of the thalamus, hypothalamus, MMBs, or periaqueductal regions. DWI and MRA showed no abnormal findings.

Three patients were excluded due to image artifacts over MMBs, and totally 8 male patients were included as controls finally (54.0 ± 1.9 years). The reasons for brain MR scan are screening ($N = 7$) and old thalamic lacunar infarction ($N = 1$). Brain MRI showed no major abnormal findings for controls except one old lacunar infarction which became almost invisible on MRI.

Susceptibility values of both MMBs were higher in cases with WKS than those in control patients (Table 1). Susceptibility values in other deep gray matters did not show major differences between cases with WKS and control patients.

Discussion

Low signal on SWI and high susceptibility values on QSM were observed for 2 cases with WKS. Our findings suggest hemosiderin depositions in MMBs for cases with WKS, and no similar finding was detected in MMBs for control patients. In the early phase of WE, in addition to abnormal hyperintensities on FLAIR, petechial hemorrhage is known to occur in MMBs with subsequent atrophy. In KS, autopsy cases and images often show hemorrhage in MMBs. QSM can provide abnormal findings of susceptibility values in MMBs, which may help us interpret the pathophysiology of WKS.

There is one previous paper reporting that susceptibility values of MMBs were around 0.05 ppm in healthy controls, which is consistent with our results for control patients.¹³ QSM showed that susceptibility values of right MMB showed significantly higher in mild cognitively impaired (MCI) patients compared with healthy controls.¹³ Susceptibility values of MMBs for cases with WKS in this study were higher than those in MCI patients.¹³ Susceptibility values of the other ROIs were not different between cases with WKS and control patients in this study; however, further studies are required to perform statistical analysis based on the limited number of cases with WKS.

There are limitations in this study. Firstly, only 2 cases with WKS are included in this study. Secondly, single-TE

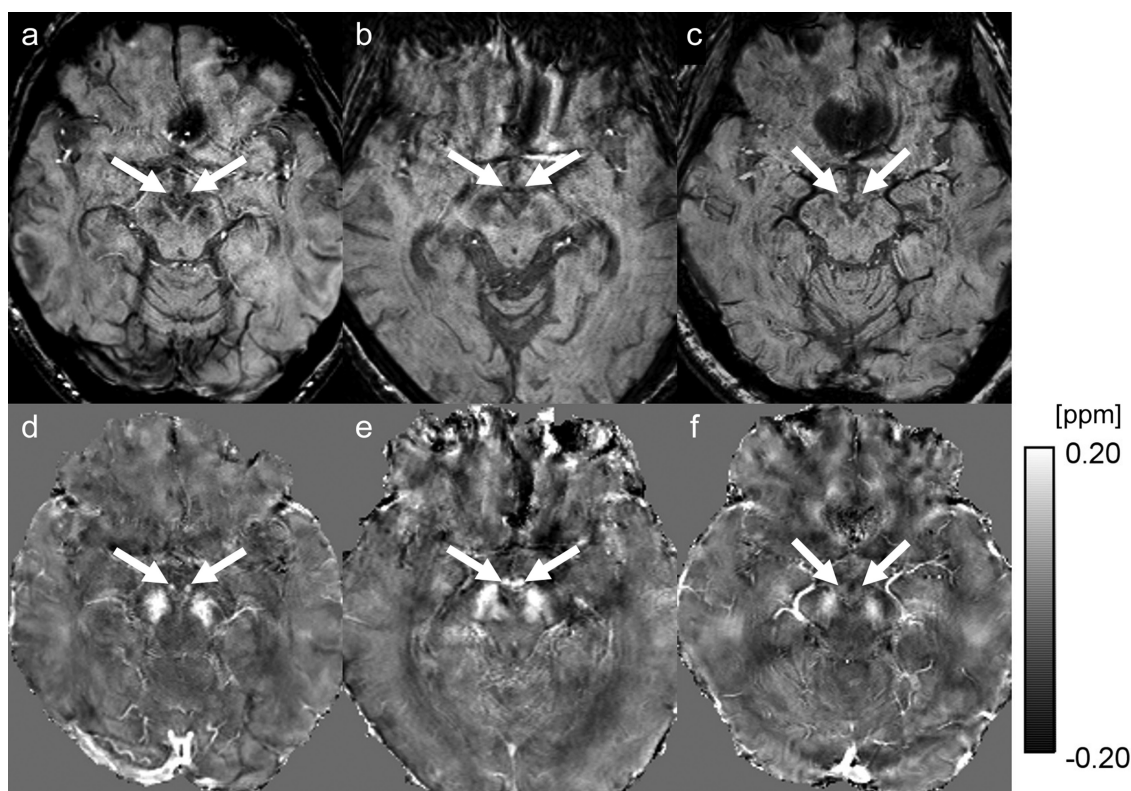


Fig. 1 SWI and QSM of case 1 (**a** and **d**), case 2 (**b** and **e**), and control patient, a 55-year-old male with dizziness and no intracranial lesions (**c** and **f**) are shown. SWI shows low-intensity spots at both MMBs in cases 1 and 2 (**a** and **b**), which correspond to high susceptibility in QSM (**d** and **e**). On the contrary, SWI shows no abnormal signal in MMBs (**c**), and QSM shows no apparent high susceptibility. Note that white arrows indicate MMBs. MMBs, mammillary bodies; QSM, quantitative susceptibility mapping; SWI, susceptibility weighted imaging.

Table 1 Mean susceptibility values (ppm) of each ROI for case 1, case 2, and 8 control patients without brain abnormalities

	Rt. MMB	Lt. MMB	Rt. GP	Lt. GP	Rt. PT	Lt. PT	Rt. SN	Lt. SN	Rt. RN	Lt. RN
Case 1	0.14	0.13	0.16	0.15	0.09	0.08	0.17	0.15	0.08	0.14
Case 2	0.19	0.18	0.20	0.20	0.10	0.09	0.22	0.14	0.08	0.14
Patients (Control)	0.06 ± 0.03	0.03 ± 0.03	0.18 ± 0.05	0.19 ± 0.05	0.08 ± 0.02	0.08 ± 0.01	0.14 ± 0.04	0.14 ± 0.03	0.12 ± 0.03	0.12 ± 0.04

Note that mean and standard deviation of susceptibility values of total 8 patients without brain abnormalities are shown in "Patients (Control)". GP, globus pallidus; Lt, left; MMB, mammillary body; PT, putamen; RN, red nucleus; Rt, right; SN, substantia nigra.

is used for this study to obtain high-resolution QSM. Single-TE QSM is susceptible to phase noise and phase unwrapping error compared to multi-TE QSM. However, good intraclass correlation coefficient was obtained between single-TE QSM and multi-TE QSM at least in deep gray matters of healthy subjects.⁷ Lastly, some motion artifacts were observed in both cases with WKS, especially in case 2. Such motion artifacts as well as susceptibility artifacts associated with paranasal sinus and skull base structures may have affected susceptibility values in this study.

In conclusion, QSM demonstrated tiny hemosiderin depositions in MMBs for cases with WKS.

Funding

This work was supported by JSPS KAKENHI Grant Numbers 21K20834, 21K15623, 21K15826, and 22K07746.

Conflicts of Interest

All authors declare that they have no conflicts of interest.

References

1. Thomson AD, Cook CC, Guerrini I, Sheedy D, Harper C, Marshall EJ. Wernicke's encephalopathy revisited. Translation

- of the case history section of the original manuscript by Carl Wernicke 'Lehrbuch der Gehirnkrankheiten für Aerzte und Studierende' (1881) with a commentary. *Alcohol Alcohol* 2008; 43:174–179.
2. Chandrakumar A, Bhardwaj A, 't Jong GW. Review of thiamine deficiency disorders: Wernicke encephalopathy and Korsakoff psychosis. *J Basic Clin Physiol Pharmacol* 2019; 30:153–162.
 3. Ota Y, Capizzano AA, Moritani T, Naganawa S, Kurokawa R, Srinivasan A. Comprehensive review of Wernicke encephalopathy: pathophysiology, clinical symptoms and imaging findings. *Jpn J Radiol* 2020; 38:809–820.
 4. Jung YC, Chanraud S, Sullivan EV. Neuroimaging of Wernicke's encephalopathy and Korsakoff's syndrome. *Neuropsychol Rev* 2012; 22:170–180.
 5. Hattingen E, Beyle A, Muller A, Klockgether T, Kornblum C. Wernicke encephalopathy: SWI detects petechial hemorrhages in mammillary bodies in vivo. *Neurology* 2016; 87:1956–1957.
 6. Ikeda T, Sakurai K, Matsukawa N, Yoshida M. Atrophic mammillary bodies with hypointensities on susceptibility-weighted images: a case-study in Korsakoff syndrome. *J Neurol Sci* 2020; 408:116551.
 7. Wicaksono KP, Fushimi Y, Nakajima S, et al. Two-Minute quantitative susceptibility mapping from three-dimensional echo-planar imaging: accuracy, reliability, and detection performance in patients with cerebral microbleeds. *Invest Radiol* 2021; 56:69–77.
 8. Oshima S, Fushimi Y, Okada T, et al. Brain MRI with quantitative susceptibility mapping: relationship to CT attenuation values. *Radiology* 2020; 294:600–609.
 9. Hinoda T, Fushimi Y, Okada T, et al. Quantitative assessment of gadolinium deposition in dentate nucleus using quantitative susceptibility mapping. *J Magn Reson Imaging* 2017; 45:1352–1358.
 10. Yamaguchi A, Kudo K, Sato R, et al. Efficacy of quantitative susceptibility mapping with brain surface correction and vein removal for detecting increase magnetic susceptibility in patients with Alzheimer's disease. *Magn Reson Med Sci* 2023; 22:87–94.
 11. Sato R, Kudo K, Udo N, et al. A diagnostic index based on quantitative susceptibility mapping and voxel-based morphometry may improve early diagnosis of Alzheimer's disease. *Eur Radiol* 2022; 32:4479–4488.
 12. Harada T, Kudo K, Fujima N, et al. Quantitative susceptibility mapping: basic methods and clinical applications. *Radiographics* 2022; 42:1161–1176.
 13. Jin Z, Sethi SK, Li B, et al. Susceptibility and volume measures of the mammillary bodies between mild cognitively impaired patients and healthy controls. *Front Neurosci* 2020; 14:572595.